



Evaluation of Laminated Composites Reinforced by High-performance Kevlar Filaments with Variable SiO₂: Mechanical, Morphological & Thermal Tests

Md. Sahab Uddin^{1,2,*}, Md. Shariful Islam³, Farjana Showline Chaity^{2,4}, Md. Ali Akbar¹, Shahin Akand^{1,5}, M. A. Gafur², A. M. Sarwaruddin Chowdhury¹

¹Department of Applied Chemistry and Chemical Engineering, University of Dhaka, Dhaka, Bangladesh

²Bangladesh Council of Scientific and Industrial Research (BCSIR), Dhaka, Bangladesh

³Department of Aeronautical Engineering, Military Institute of Science and Technology (MIST), Dhaka, Bangladesh

⁴Department of Microbiology, Noakhali Science and Technology University, Noakhali, Bangladesh

⁵Department of Chemistry, Gaibandha Mohilla College, Gaibandha, Bangladesh

Email address:

sihab.bcsirtg@gmail.com (Md. S. Uddin)

*Corresponding author

To cite this article:

Md. Sahab Uddin, Md. Shariful Islam, Farjana Showline Chaity, Md. Ali Akbar, Shahin Akand, M. A. Gafur, A. M. Sarwaruddin Chowdhury. Evaluation of Laminated Composites Reinforced by High-performance Kevlar Filaments with Variable SiO₂: Mechanical, Morphological & Thermal Tests. *Composite Materials*. Vol. 4, No. 2, 2020, pp. 15-24. doi: 10.11648/j.cm.20200402.11

Received: August 12, 2020; **Accepted:** August 24, 2020; **Published:** September 16, 2020

Abstract: In contemporary years, a necessity to produce satisfactory and progressive modules for engineering roles have been expanded rapidly. Laminated fiber-strengthened composite substances have well-made candidature for satisfying those factors with huge applications in nearly all regions of engineering and technology. Glass, Carbon, and aramid fibers are using extensively for the manufacturing of fiber-bolstered polymer composites. Kevlar is the highly accepted aramid fiber having an extended chain of strong, ring-like aromatic molecules. Superior temperature and shock-resistant aspects make kevlar the maximum promising antiballistic fabric with balance at elevated temperatures. It is extensively used for human body armor panels for light-weight army vehicles, bulletproof jackets, and fireproof bodysuits, and in aerospace industries, etc. In this work, we tested the tensile, flexural, and impacts strength of kevlar 49 (K-49) fiber-reinforced polymer complex. We additionally characterized its DTG/TG test, FTIR test, and SEM analysis for a definite and reliable notion of it. The composite samples used on this work had been organized with the aid of using hand lay-up procedure. All Mechanical characterizations had been carried out according to the necessities of ASTM standards. In this study, highest tensile strength and elastic modulus was observed for 5*% milled silica and lowest for composite with 0% silica. Composite C4 of 2% silica shows the maximum hardness in both Leeb rebound and Vickers micro hardness method (320.1HV, 447.8HRC). DTG curves of composites show that at 378.8°C, and 355.5°C the rate of degradation of the composite was 559 µg/min, and 58.5µg/min for composite C1, and C7 respectively. However, the findings were supported by FTIR and SEM images analysis.

Keywords: Kevlar, Laminated Composite, Tensile Strength, Flexural Strength, Water Absorption, Hardness, FTIR, SEM

1. Introduction

Composites are made of multiple components that are chemically distinctive with a definite boundary between them. In a hybrid composite, multiple discontinuous phases are embedded in a continuous phase; the discontinuous phase is termed as hybrid reinforcement as it is stronger and harder than the continuous phase which is termed as a matrix [1].

Fiber-reinforced polymer composites are being used in a number of sectors due to their properties like environmental tolerances, strength, and stiffness. The Kevlar is a polymeric fiber with low density, high tensile strength, and lightweight. Despite having light weight, it can withstand more (five times) impact resistance than the steel in the same weight [2-

4]. Kevlar composites have been used in several applications due to their impact resistance properties. This synthetic fiber has been employed extensible in military helmets [5-8]. Low-molecular-weight pre-polymers like epoxy resins have multiple epoxide groups; these are widely used in fiber-reinforced materials. Diglycidyl ether of bisphenol-A, a type of epoxy resin is often used as a building block and starting materials for different types of materials [9, 10]. Mourad et al. have recently investigated the effect of nanofiller-reinforced Kevlar /epoxy resin laminated composites. Nanofillers employed in the fabrication were silicon carbide, aluminum oxide, and multiwalled carbon nanotube [11]. Besides statistical simulations were carried out by Kumar et al. to evaluate the performance of Kevlar/epoxy composite sheets [12]. In another study, carbon nanotubes were added to Kevlar-ultrahigh molecular weight polyethylene fiber hybrid composites [13]. A recent study by Sharma et al. revealed that the incorporation of multi-walled carbon nanotube in the Kevlar composite increased the tensile strength to 350 MPa which is an increase of about 90% over the pristine fiber [14]. An increased amount of interface are provided by the MWCNT was responsible for this enhanced mechanical properties [15]. Incorporation of carbon fiber to Kevlar/epoxy composite was also studied by Al-qabandi et. al. [16]. A lot of researchers investigated the mechanical properties of glass and carbon fiber-reinforced composites [17-19]. In the present work, K-49 aramid fiber is used as a reinforcement filler for epoxy-based polymer composite. Samples were prepared as laminated composite panels under room temperature; the tensile strength, flexural strength, impact strength, and hardness of composite samples along with DTG/TG, FTIR, and SEM analysis were investigated. All tests were performed according to their respective American Society of Testing and Methods (ASTM) standards.

2. Experimental

2.1. Materials

The reinforcement used in this study was woven Kevlar® fiber (Type - 1F537, density-1.41 g/mm³; diameter-14 m; average length-1.7 mm; Young's modulus-56.2 GPa; Poisson ratio- 0.37) [20]. The matrix was E-51 epoxy resin (bisphenol-A) and resin hardener (4 methyl -1, 2, 3, 6-tetrahydro phthalic anhydride) with crystalline industrial grade silica (SiO₂). Silica was milled in planetary ball mill for size reduction.

2.2. Fabrication of Composite

Several steps are involved in the composite fabrication process, (a) Weighing of raw materials, (b) Treatment of Fabrics, (c) Sandwich like composite preparation (d) Hydraulic Pressing, and (e) Sizing for the desired test [21]. In this work, we used Kevlar 49 as reinforced in fabric and sheet form. Kevlar was cleaned by dipping in ethanol to make the fabric more oriented. Raw Kevlar was cut into 10x10 cm length and width. Then these fibers were weighed in a digital balance. After drying in a vacuum dryer for 1 hour

at 80°C, the sample was cooled in a desiccator. The hand lay-up process was used to fabricate all composite in this study. A mold releasing agent was also used on the mold surface to remove the composite easily after the completion of fabrication. Seven composite sheets were fabricated in the ratio of 0% (Kevlar-Epoxy+ 0% SiO₂), 0.5%, 1%, 2%, 2*%, 5%, 5*% by weight of the matrix. Then the composite sheet was arranged as a sandwich of fabric sheet (3 layers) and matrix. The curing agent was added to the resin and the composite was then compressed in the hydraulic press's lower plate for 24 hr. at room temperature with 100KN pressure. After 24 hours of treatment, the composite was then removed out of the mold to cut it in the desired shape. All test specimens were machined from the cured composite plates as per requirement. Here * indicate the composition with milled silica.

2.3. Major Equipment's Used for the Fabrication of Sample

Equipment (Figure 1) used for the preparation of composite were: W/P Hydraulic Press machine, Oven, Planetary ball mill, and Molds.



Figure 1. Photographic image of the instrumental set-up (a) Vacuum oven (b) planetary ball mill (c) W/P hydraulic press machine.

3. Characterization

3.1. Bulk Density and Water Uptake Test

A bulk density specimen was prepared according to the ASTM C135-76 and the bulk density of the specimen in grams per cubic centimetre was calculated using the following formula: $D=WS/V$. A schematic diagram of the block-on-ring type friction and wear tester used in this study is shown in figure 2 (d). Water uptake test specimen for the composite was prepared according to ASTM Design: 570-81 (Reapproved 1988 {ASTM Design: D570-81 Standard test method for water absorption of plastic [22]. The test specimen was 10mm wide and 40mm long which machined with a mechanical stainless steel blade rotor with rpm 18,000. The cut edge was made by finishing with emery paper, dried in the oven for 24hr at about 50°C and then Cooled in a desiccator and immediately weighted by a microbalance. Then placed in a container of distilled water (23°C) and kept there for 24 hr. Then the specimen was removed one at a time, wiped the surface with a tissue paper and immediately weighted by microbalance. Test specimen prepared for the Water absorption test are shown in figure 2 (d).

3.2. Tensile Strength

The tensile test method is designed to produce tensile

property data for the control and the specification of plastic material [23]. The tensile specimen was prepared for this study according to ASTM-638M-91a [24]. The test specimen was 10.5 mm wide and 90mm long with 2mm in thickness

which was machined with a mechanical stainless-steel blade rotor (rpm- 18,000). The test speed of UTM was 1mm/min. Test specimen prepared for the tensile strength test are shown in figure 2 (a).

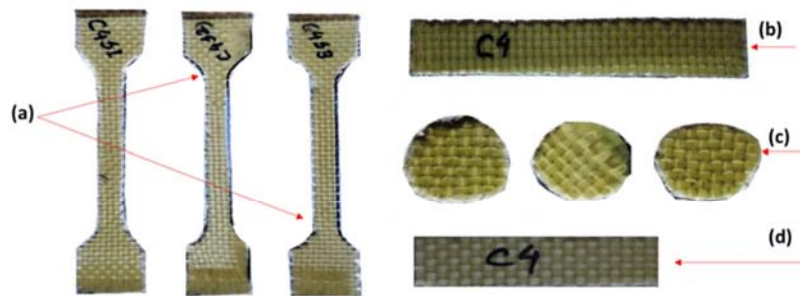


Figure 2. Specimen prepared for (a) tensile test (b) flexural strength (c) hardness (d) water uptake test.

3.3. Flexural Strength

The flexural specimen of the Kevlar-epoxy composite was prepared according to ASTM D790M, 3 point loading [25]. The test specimen prepared for tensile strength are presented in figure 2 (b). The specimen dimension was (60x10x1.4) mm³ and the support span was 45 mm. The test speed was taken as 2 mm/min. Flexural strength was calculated at point of load-deflection utilizing the following equation: $S=3PL$ [26].

3.4. Hardness

A circular specimen of composite with a 1 cm radius used for the hardness test of the composite is shown in figure 2 (c). According to the Leeb dynamic principle, the hardness test is derived from the power loss of a described impact physique. The Leeb fraction (v_i , v_r) is taken as the extent of loss of energy by plastic distortion: the impact body ricochets faster from stiffer test samples than it does from laxer ones, resulting in a greater assessment $1000 \times v_r/v_i$. Instead, the microhardness of the samples was measured by using the following formula: $HV=1.854 \times L/d^2$ [27].

3.5. Fourier Transformed Infrared Spectroscopy (FTIR)

The functional group analysis of our composite was conducted by Fourier Transform Infrared Spectroscopy. FTIR is an effective device for figuring out the forms of chemical bonds in a molecule with the aid of using generating an infrared absorption spectrum like a molecular “fingerprint” [28]. Infrared radiation spectra give the graph of % transmittance vs wavenumber. Small amounts of sample were mixed with KBr powder for making the transparent sheet. The FTIR spectra was recorded with FTIR, Model: Shimadzu FTIR-8400S, Range: 4000 – 700 cm⁻¹; Resolution: 4 cm⁻¹; No of scans: 20 times.

3.6. SEM Analysis

The surface morphology of the fractured surface of samples was observed by using Scanning Electron Microscope (SEM), in the Centre for Advanced Research in Sciences (CARS), University of Dhaka, Model: JSM-

6490LA. The JSM-6490LA is a high-performance scanning electron microscope with an embedded energy dispersive X-ray analyzer (EDS) which allows for seamless observation and EDS analysis. It has a high resolution of 3.0 nm and 500X. SEM image analysis of our composite was important for the observation of surface morphology, particle size, particle distribution, porosity, and pore size.

3.7. TG/DTG Analysis

A thermal analysis of composites was carried out to measure the stability of composite with increasing temperature. TG stands for Thermo-gravimetry and DTG for Differential Thermo-gravimetry which indicates % wt. loss and rate of wt. loss of composite with increasing temperature and time respectively. A Shimadzu TG/DTG analyzer of Model TG/DTGA6300 was used where, maximum temperature: 1000°C, Sample: 3.581 mg, and reference: 2.830 mg (alumina).

4. Results and Discussion

4.1. Physical Properties of Composite

4.1.1. Bulk Density

Figure 3 shows the effect of variation of filler in the bulk density of Kevlar® reinforced Epoxy composites. The bulk density of the composites initially increases with the increment of quartz and peaks at 2% and then decreases. For composite C1 it was 0.00110 (gm./mm³) and at 2% load of silica in C4 it became 0.00171 (gm/mm³) and then decreased with filler addition. Due to the presence of pores in composite, the increment of filler loading mass increased rapidly than its volume, which therefore increases the overall density of composites up to C4. After the saturation of pore volume density remains constant with excess filler addition. Bulk density increment means the composite becomes denser. So, for heavy load applications, composite with 2% filler is more applicable.

4.1.2. Water Uptake Test

Water immersion tests were carried out on the composite samples to study the effects of water absorption on the

mechanical properties. It has a great impact on the tensile and flexural properties of the composite. Several wt. percent of quartz has been taken for the fabrication of composites. The effect of immersion time and filler addition on water absorption of the kevlar-epoxy composite is shown in figure

4. Water absorption of Kevlar-Epoxy composite samples was monitored at 25°C and it revealed that the water absorption depends on filler content and immersion time. The time-bound test data of water absorption of the composite are represented in table 1.

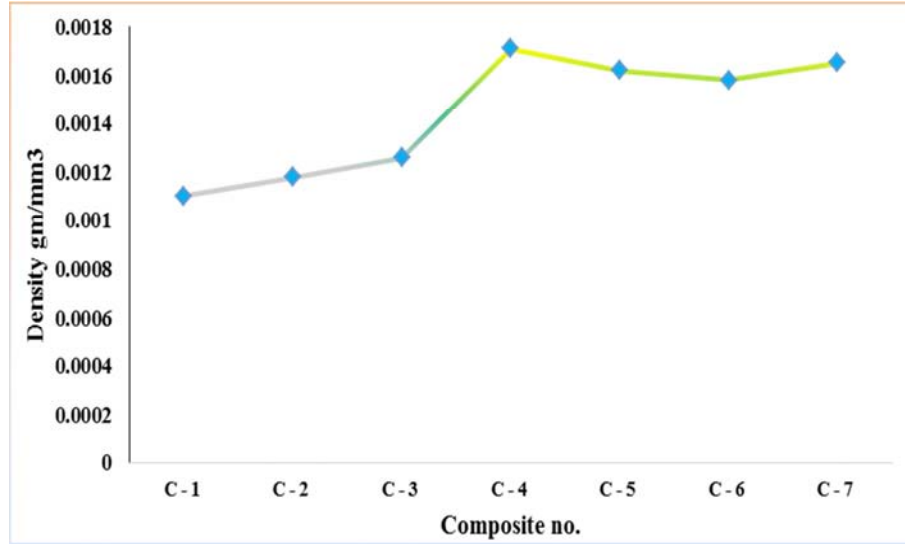


Figure 3. Effect of amount of quartz addition on the bulk density of laminated composite.

Table 1. Test data of water absorption of composite with variable time.

Sample	% of water uptake				
	0 hr	1 st day	3 rd day	5 th day	7 th day
Kevlar-Epoxy+ 0% SiO ₂	0	7.56	8.23	9.37	9.98
Kevlar-Epoxy +.5% SiO ₂	0	5.19	8.55	9.54	9.78
Kevlar-Epoxy+ 1% SiO ₂	0	3.19	5.13	5.96	6.65
Kevlar-Epoxy+ 2% SiO ₂	0	2.70	6.47	7.29	7.96
Kevlar-Epoxy+ 2*% SiO ₂	0	2.60	4.46	5.07	5.84
Kevlar-Epoxy+ 5% SiO ₂	0	2.48	3.71	4.13	4.53
Kevlar-Epoxy+ 5*% SiO ₂	0	2.30	4.73	5.24	6.52

Results show that the water absorption values decrease with increasing filler content where time is the same for all composite. After 24hr, for composite with 0% filler, water intake percentage was maximum at 7.56%, wherewith the increase of filler it becomes 2.30% for composite with 5% SiO₂. This phenomenon happened because increase filler

content reduced the porosity or voids in the composite which cause less absorption of water. Point to be noted that, due to the presence of a large amount of OH- group in matrix originated from the crosslinking of Epoxy and TETA, the initial amount of percent water absorption was high.

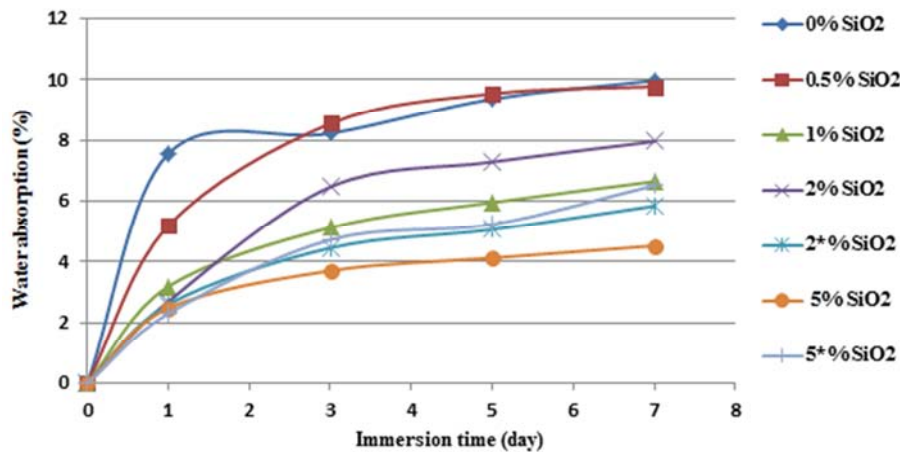


Figure 4. Water uptake scenario of Kevlar-epoxy composite based on time.

4.2. Mechanical Properties of Composite

4.2.1. Tensile Strength & Elongation Percentage

The tensile test is the most vital test for composites especially those composites fabricated for structural purposes. For the tensile test of my composite tensile specimen was prepared according to ASTM-638M-91a (90*10.5*2) mm

[29]. The Ultimate Tensile Strength, Elongation, and Elongation at Yield of kevlar-epoxy resin composite specimen were determined by the UTM machine. Table 2 represented the Tensile Strength, percentage Elongation data read out from the UTM machine.

Table 2. Tensile strength and elongation percentage data of laminated composite.

Composite no.	Sample	Elongation %	Tensile strength (MPa)
C1	Kevlar-Epoxy+ 0% SiO ₂	17.23	153.7
C2	Kevlar-Epoxy + 0.5% SiO ₂	23.96	248.0
C3	Kevlar-Epoxy+ 1% SiO ₂	21.96	263.0
C4	Kevlar-Epoxy+ 2% SiO ₂	20.86	286.1
C5	Kevlar-Epoxy+ 2*% SiO ₂	19.77	320.1
C6	Kevlar-Epoxy+ 5% SiO ₂	16.50	400.0
C7	Kevlar-Epoxy+ 5*% SiO ₂	14.69	411.6

Figure 5 shows UTM graphs of the tensile strengths of the composites for Kevlar-Epoxy with 0% SiO₂ and Kevlar-Epoxy with 5*% SiO₂. It is observed that the value of UTM was highest for 5*% milled silica and lowest for composite with 0% silica. For Composite-1 which consists of 0% silica, the ultimate tensile strength was 153.7 and it reached 411.6 with the increment of filler quartz. Numerous researchers have revealed that the amalgamation of particulate in composite matrix effects in successively improved mechanical strength at a definite amount of filler loading.

Tensile strength increases with the increase in the percentage of silica and was highest for milled silica. It is assumed that with the increase of silica in composite filled up voids and cavities of the matrix. As a result, it improves the total load-bearing capacity as well as the Ultimate Tensile Strength of composite. Epoxy resins shrink considerably after curing which hamper fiber alignment in composite causing low strength. Here, filler reduces this shrinkage and maintains the uniform distribution of load along with the specimen.

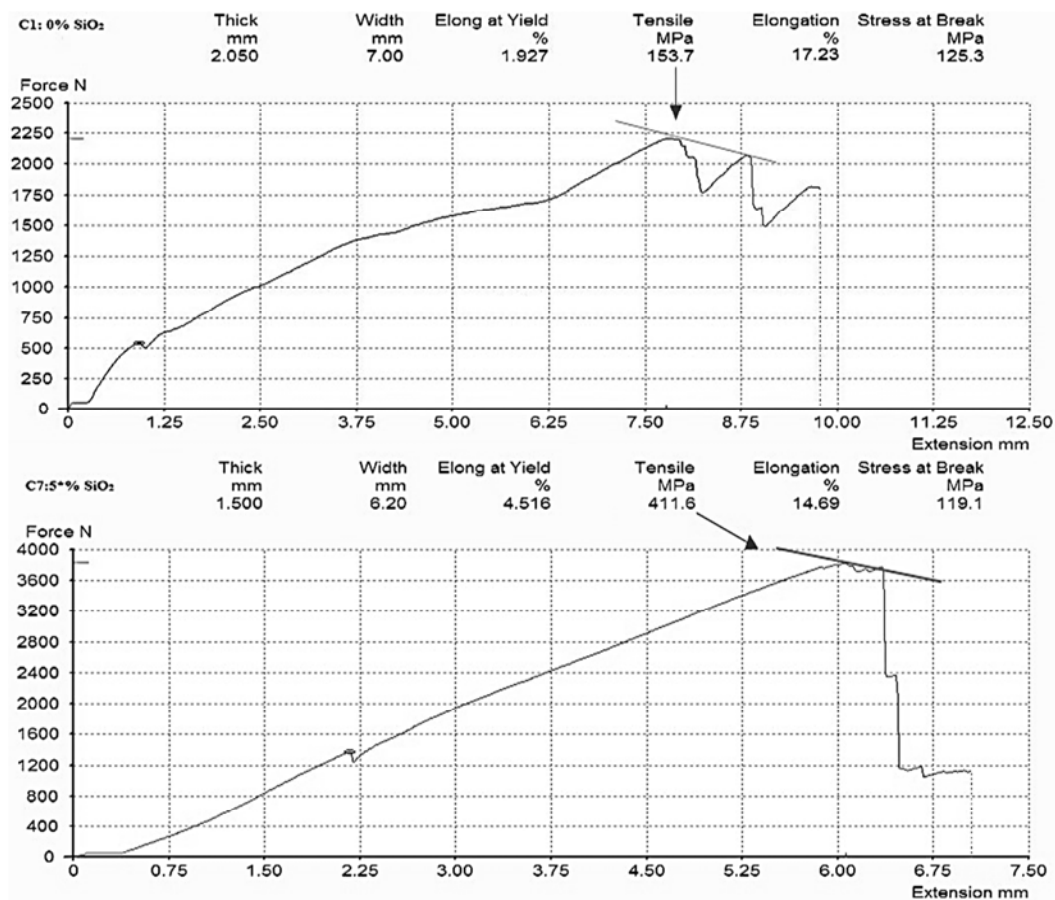


Figure 5. UTM curve for Kevlar-Epoxy with 0% SiO₂ (C1) and Kevlar-Epoxy with 5*% SiO₂ (C7).

Here, *figure 6* shows the percent elongation of the composites on different composition of quartz. The highest value of percent elongation for the Kevlar-epoxy composite was found in 0.5% silica and lowest value for kevlar-epoxy with 5% milled SiO₂. Percent elongation decrease with the increase of tensile strength of the composite, i.e. percent elongation decreases with the addition of SiO₂.

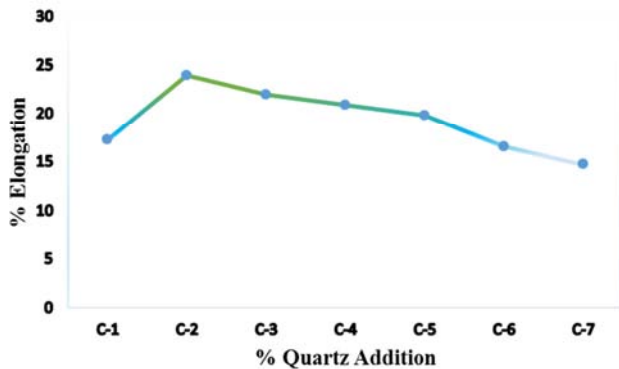


Figure 6. Effect of filler on Elongation of laminated Kevlar- epoxy composite.

4.2.2. Flexural Test and E-Modulus

Flexural test of specimen measures the behavior of materials subjected to beam loading. It is likewise referred to as a transverse beam test with a few materials. Maximum fiber strain and maximum pressure are calculated for increments of load. The specimen dimension was (60*10*1.4) mm³ and the support span was 45 mm. *Figure 7* illustrates the effect of the addition of quartz on the flexural strength of the kevlar-epoxy composite. It reveals that the flexural strength of composite increased with the increment of silica and it became maximum for 2% milled silica addition. In composite C1 the flexural strength was 33.11MPa and with the addition of silica, it goes to 77.70MPa. From these results, we can infer that with the increase of silica in composite it filled up voids and cavities of the matrix and it also managed good fiber orientation in the matrix. As a result, it improves the total load-bearing capacity as well as the flexural strength of the composite. The flexural strength of the composites is greater than kevlar-epoxy, so these composites are less brittle. Ceramic materials are brittle and strong in compression but weak in shearing and tension. The flexural and bending modulus of a composite is the proportion of stress and strain in flexural distortion or affinity of a material to twist.

Here, *figure 8* shows that the flexural E-Modulus increases with the increment of silica and was maximum in C5 and then decrease. The increase in the volume fraction of filler reduces cavities formed in the composite and this can explain the increment E-Modulus. And after saturation of filler excessive filler addition makes it fragile that is why in C6 and C7 E-Modulus decreases. So, from these data, we can incur that for the fabrication of beam with this composite C5 is the best choice.

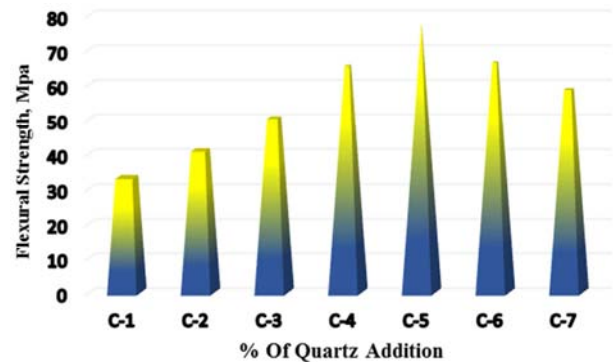


Figure 7. Effect of quartz addition on Flexural strength.

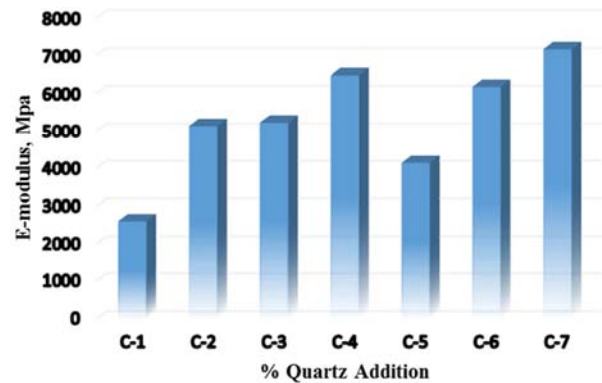


Figure 8. Effect of quartz addition on E-Modulus of flexural strength.

4.2.3. Hardness of Composites

Hardness is the property of a composite to resist indentation or penetration of a substance on a composite surface. A Micro Hardness tester (Model HMV-2) and a Leeb Rebound Hardness Tester (Model H1000) was used for measuring the hardness of the composite. In Micro Hardness tester test load was 4.903 N. In our study we found that the filler addition does not return any harmonic result. So, spotting the result displayed in *figure 9* shows that the filler addition has less effect on the hardness of the composite. According to Leeb-Rebound test hardness was maximum for C1 (461.2 HRC) wherein the Vickers Hardness test was maximum for C4 (320.1HV). Therefore, composite C4 of 2% silica shows the maximum hardness in both methods. Composite C4 of 2% silica shows the maximum hardness in both method (320.1HV, 447.8HRC).

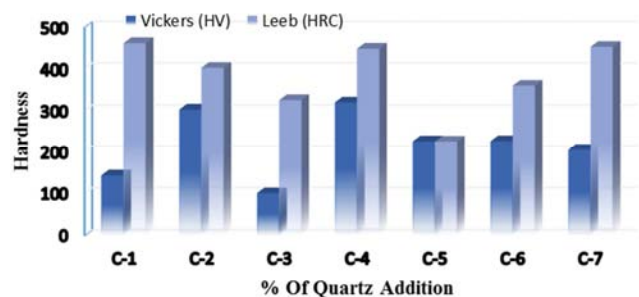


Figure 9. Effect of addition of filler on the Hardness of composites.

4.3. Morphological Analysis

4.3.1. SEM Analysis

Figure 9 (C1) show magnified images of the composite surface at 50 μm and 500X magnification. Few voids are evident at 50 μm and 500X magnification of C1 composite. It proves the incapability of fiber surface with matrix, which

results in poor adhesion between fiber and matrix of the composites. But figure 10 (C7) displays a smooth surface which indicates a homogeneous morphology of composite even at 500 magnifications. It has fewer voids than composites C1. It may be happened due to the increment of filler percentage.

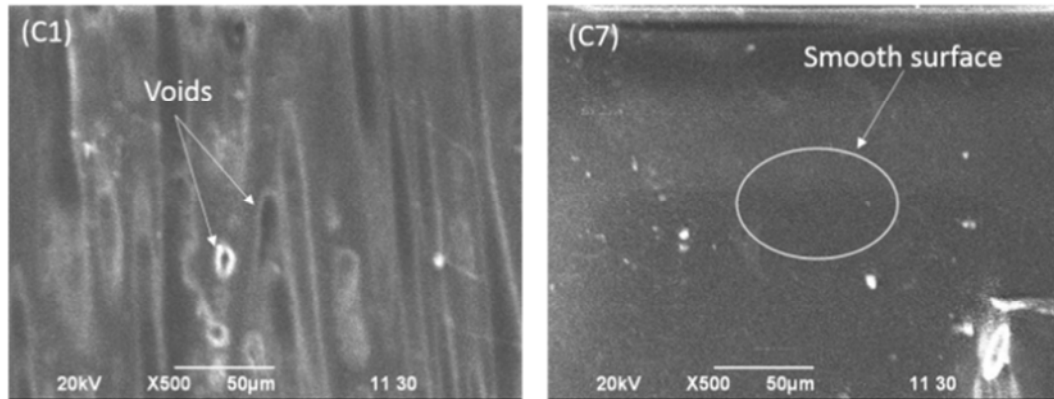


Figure 10. SEM image of composite surface of C1 and C7 at 50 μm and 500X magnification.

Figure 11 visualizes the fiber orientation of composite at fracture and delaminated surface when images were taken at 50 μm and 500 times magnification. Fiber is displaced here may because of high hydraulic pressure (100KN). Here we found that fiber in C7 is more oriented than C1. Epoxy resins shrink considerably after curing, this shrinkage reduces the

specific volume of the matrix and it results in free spaces between matrix and fiber. Which finally effects haphazard fiber orientation in the composite. The addition of filler reduces this shrinkage property and makes fiber arrangement more oriented, which evident in figure 11 (C7).

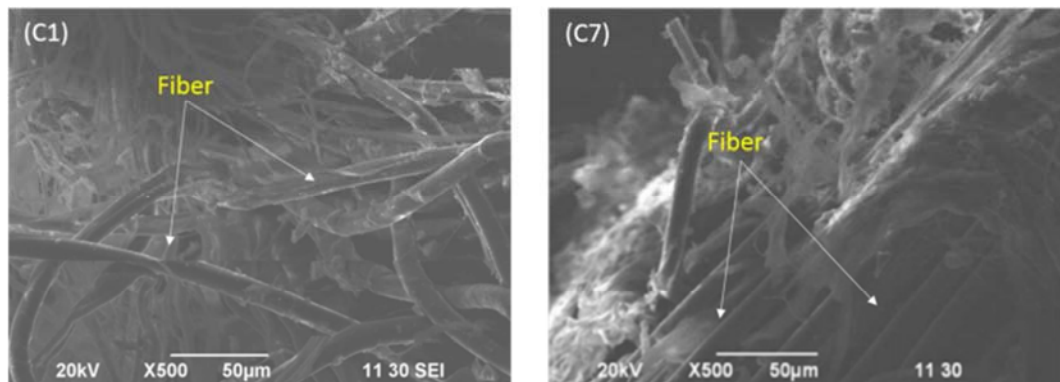


Figure 11. Fiber orientation of composite C1 and C7 at 50 μm and 500X magnification.

4.3.2. FTIR Analysis

FTIR is a potential appliance for detecting the types of chemical bonds in a compound by generating an infrared absorption band. Figure 12 shows the FTIR spectrum of Kevlar Fiber. The major peaks are found in the region of 821.68 cm^{-1} , 1311.56 cm^{-1} , 1523.76 cm^{-1} , 1641.42 cm^{-1} and 3327.21 cm^{-1} , corresponding to the bond C-H in the ring, C-N Stretching, C=C Stretching in the ring, C=O Stretching of amide, N-H Stretching. FTIR profile of matrix (Epoxy-Resin) is shown in figure 13 It shows that major peaks are found in 771.53 cm^{-1} , 827.46 cm^{-1} , 1035.77 cm^{-1} , 1242.16 cm^{-1} , 1508.33 cm^{-1} , 1643.63 cm^{-1} , 2924 cm^{-1} and 3813.27 cm^{-1} corresponding's to Rocking $-\text{CH}_2$ in the polymer chain,

Stretching C-O-C in oxirane group, Stretching C-O-C in ether, Stretching C-N of amine link, Stretching C-C of the aromatic ring, Stretching C=C of the aromatic ring, Bending N-H of $-\text{CH}_2-$ and for free -OH Group. From the FTIR spectrum of composite in figure 14 it is observed that only significant change occurs in composite at 3200-3500 cm^{-1} and 3600-4000 cm^{-1} region which may be for H-bonded and free -OH group formed in the composite. Another most significant change observed in the spectrum is that a cave is found in 1650 – 1850 cm^{-1} region i.e. % of the transmittance of infrared light increased in composite with the increase of crystalline silica.

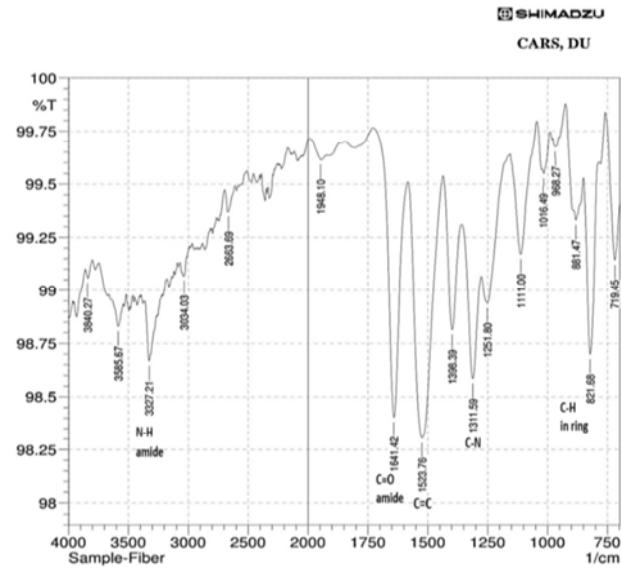


Figure 12. FTIR Spectra of kevlar fiber for frequency region 750-4000 cm^{-1} .

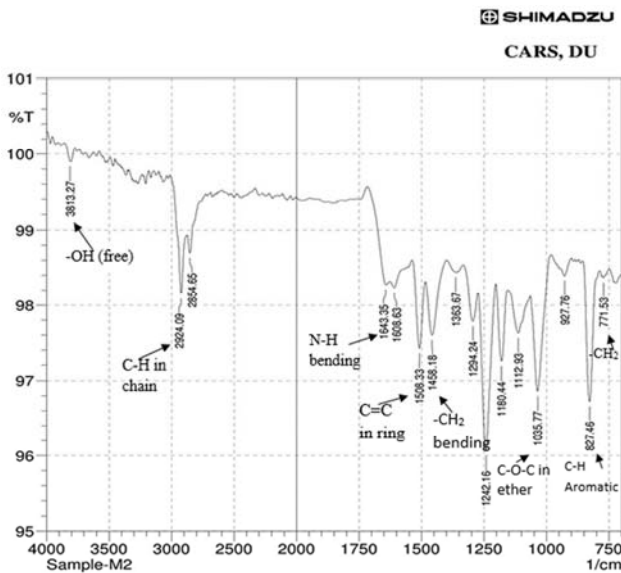


Figure 13. FTIR Spectra of Matrix (Epoxy-resin) for frequency region 750-4000 cm^{-1} .

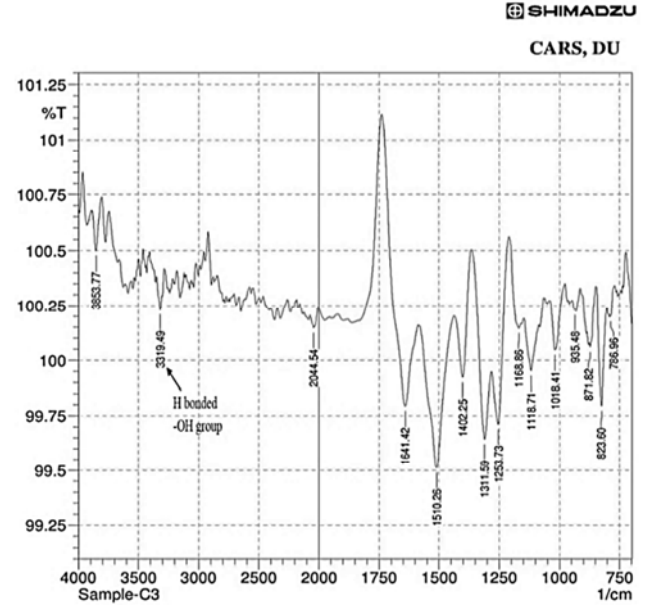


Figure 14. FTIR Spectra of Sample (Kevlar-Epoxy with 1% SiO₂) for frequency region 750-4000 cm^{-1} .

4.4. Thermal Analysis (TG/DTG)

Figure 15 illustrate the Thermo Gravimetric (TG) and Differential Thermo Gravimetric (DTG) curves of filler silica and kevlar fiber. The top (blue) one is the TG and the Bottom (red) one is the DTG. Figure 15 (a) indicates that 7.4% weight loses at 438°C in a fiber sample due to moisture. Then again, the DTG curve shows that the maximum degradation occurs at only 601°C with a rate of 0.734 mg/min. On the other hand, the TG curve in figure 15 (b) shows that the major degradation occurs at one stage for the silica. Initially, it loses 16.0% of its weight at 295°C due to moisture. Then the TG curve reveals that the onset temperature of silica was 446°C and 50% degradation occurs at 475°C. The total degradation loss is 57.1%. The DTG curve shows that the maximum degradation occurs temperature of 463°C with a rate of 0.337 mg/min.

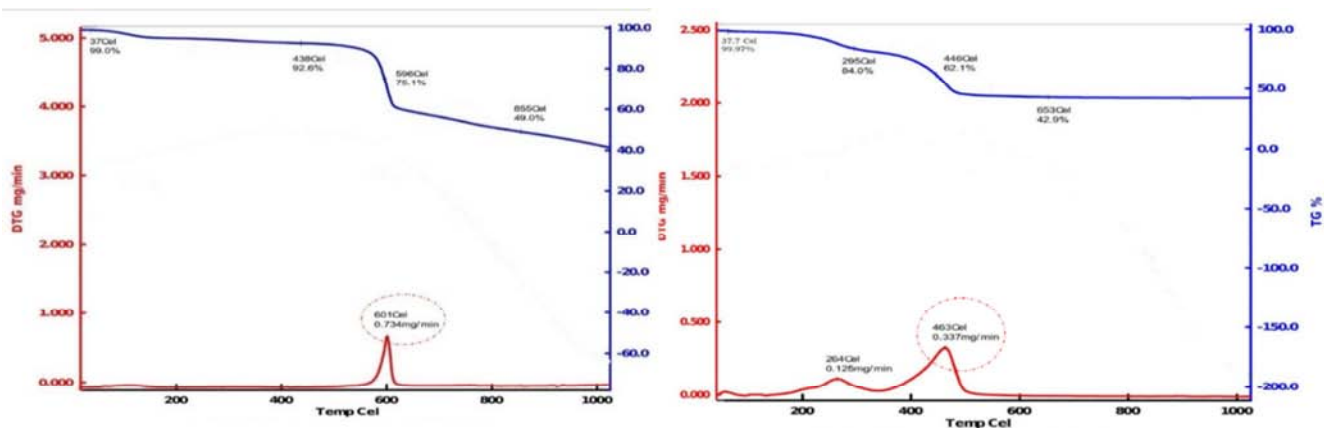


Figure 15. TG and DTG curves for (a) kevlar fiber (b) crystalline silica particle (SiO₂).

From figure 16 (a) it is observed that for all composite weight loss starts at around 220°C. For composite C1 it was 6.7% at 242°C and in composite C7 it goes to 4.6%. This is mainly for the initial exclusion of moisture from composite material. Major degradation for all composite starts at around 300°C and degradation was maximum at 1000°C. Composite C1 shows maximum degradation loss 83.4% at 546°C and in composite C7 it becomes 22.9%. These types of degradation occur mainly for the combustion of material at elevated

temperatures. From these TG curves, it is clear that the increment of filler reduces the degradation loss of composites i.e. it improves the thermal stability of composite much more. Again, the DTG curves (above) of composites show that at 378.8°C, and 355.5°C the rate of degradation of the composite was 559 µg/min, and 58.5µg/min for composite C1, and C7 respectively. This indicates that the gradual addition of silica reduces the rate of weight loss of composite (figure 16 (b)).

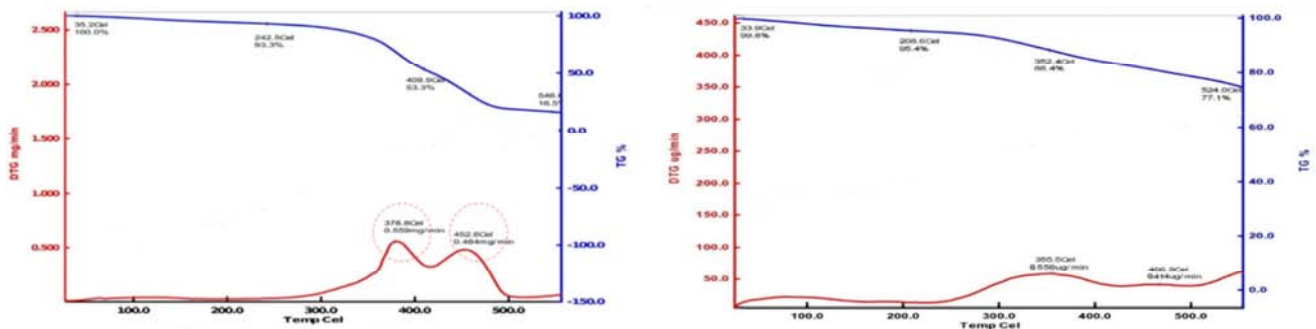


Figure 16. TG and DTG curves for composite C1 at variable temperature, (0 - 600°C).

5. Conclusion

The experimental characterization and analysis of different properties of Kevlar-Epoxy composites with silica lead us to some precise decision. Tensile and flexural strength of Kevlar-Epoxy composites was increased constantly with an increase of silica content but decreased after 2% milled silica addition. Alternatively, it was also observed that the elongation percentage decreased with increasing filler addition. So, we can say, excessive filler does not increase mechanical properties else it may cause negative results in the composite. TG and DTG curves of composites show that the degradation of composites was occurring at only one stage which exhibit that kevlar-epoxy composites possess good thermal stability. From spectral analysis it was observed that, additional peak appears only at 3200-3500 cm^{-1} & 3600-4000 cm^{-1} region which may be for newly formed H-bond and free -OH group. The images of the Scanning Electron Microscope displayed that the surface morphology of some composite was not uniform, and the number of cavities were decreased with the increase of filler. Finally, we can conclude that, for heavy load application composites of good strength could be successfully developed by using 2*% (milled, particle size: 19.4 µm) silica as a filling agent. On the other hand, for high thermal application, composite with high filler content (5*% SiO_2) is more suitable than Composite C5 (2*% SiO_2).

Conflict of Interest

The authors declare that they have no competing interests.

Funding

This research did not receive any specific grant from funding agencies in the public or commercial sectors.

Acknowledgements

We thank Bangladesh Council of Scientific and Industrial Research (BCSIR) for giving access to the laboratory facilities.

References

- [1] Sathishkumar, T., Satheeshkumar, S. and Naveen, J. Glass fiber-reinforced polymer composites—a review. *Journal of Reinforced Plastics and Composites*, 33, 13 (2014), 1258-1275.
- [2] Roberts, G. D., Pereira, J. M., Braley, M. S., Dorer, J. D. and Watson, W. R. Design and testing of braided composite fan case materials and components (2009).
- [3] Tham, C., Tan, V. and Lee, H.-P. Ballistic impact of a KEVLAR® helmet: Experiment and simulations. *International Journal of Impact Engineering*, 35, 5 (2008), 304-318.
- [4] Ebrahimnezhad-Khaljiri, H., Eslami-Farsani, R. and Akbarzadeh, E. Effect of interlayer hybridization of carbon, Kevlar, and glass fibers with oxidized polyacrylonitrile fibers on the mechanical behaviors of hybrid composites. *Proceedings of the Institution of Mechanical Engineers, Part C: Journal of Mechanical Engineering Science*, 234, 9 (2020), 1823-1835.
- [5] Walters, W. and Scott, B. High velocity penetration of a Kevlar reinforced laminate. *Proc. Of the 22nd SAMPLE Int'l Tech. Conf.* (1990) 1078-1091.

- [6] Bandaru, A. K., Chavan, V. V., Ahmad, S., Alagirusamy, R. and Bhatnagar, N. Ballistic impact response of Kevlar® reinforced thermoplastic composite armors. *International Journal of Impact Engineering*, 89 (2016), 1-13.
- [7] Park, B., Lee, W., Lee, E., Min, S. H. and Kim, B.-S. Highly tunable interfacial adhesion of glass fiber by hybrid multilayers of graphene oxide and aramid nanofiber. *ACS applied materials & interfaces*, 7, 5 (2015), 3329-3334.
- [8] Lian, M., Fan, J., Shi, Z., Li, H. and Yin, J. Kevlar®-functionalized graphene nanoribbon for polymer reinforcement. *Polymer*, 55, 10 (2014), 2578-2587.
- [9] Jin, F. L., Ma, C. J. and Park, S. J. Thermal and mechanical interfacial properties of epoxy composites based on functionalized carbon nanotubes. *Materials Science and Engineering: A*, 528, 29-30 (2011), 8517-8522.
- [10] Zhu, L., Jin, F.-L. and Park, S.-J. Thermal stability and fracture toughness of epoxy resins modified with epoxidized castor oil and Al₂O₃ nanoparticles. *Bull Korean Chem Soc*, 33 (2012), 2513.
- [11] Mourad, A.-H. I., Idrisi, A. H., Zaaroura, N., Sherif, M. M. and Fouad, H. Damage assessment of nanofiller-reinforced woven kevlar KM2plus/Epoxy resin laminated composites. *Polymer Testing* (2020), 106501.
- [12] Kumar, S., Gupta, D. S., Singh, I. and Sharma, A. Behavior of kevlar/epoxy composite plates under ballistic impact. *Journal of Reinforced Plastics and Composites*, 29, 13 (2010), 2048-2064.
- [13] Bigdilou, M., Eslami-Farsani, R., Ebrahimnezhad-Khaljiri, H. and Mohammadi, M. A. Experimental assessment of adding carbon nanotubes on the impact properties of Kevlar-ultrahigh molecular weight polyethylene fibers hybrid composites. *Journal of Industrial Textiles* (2020).
- [14] Sharma, S., Pathak, A. K., Singh, V. N., Teotia, S., Dhakate, S. and Singh, B. Excellent mechanical properties of long multiwalled carbon nanotube bridged Kevlar fabric. *Carbon*, 137 (2018), 104-117.
- [15] Sharma, S., Kumar, V., Pathak, A. K., Yokozeki, T., Yadav, S. K., Singh, V. N., Dhakate, S. and Singh, B. P. Design of MWCNT bucky paper reinforced PANI-DBSA-DVB composites with superior electrical and mechanical properties. *Journal of Materials Chemistry C*, 6, 45 (2018), 12396-12406.
- [16] Al-Qabandi, O., De Silva, A., Al-Enezi, S. and Bassyouni, M. Synthesis, fabrication and mechanical characterization of reinforced epoxy and polypropylene composites for wind turbine blades. *Journal of Reinforced Plastics and Composites*, 33, 24 (2014), 2287-2299.
- [17] Tseng, H.-C., Chang, R.-Y. and Hsu, C.-H. Numerical prediction of fiber orientation and mechanical performance for short/long glass and carbon fiber-reinforced composites. *Composites Science and Technology*, 144 (2017), 51-56.
- [18] Sprenger, S. Improved performance of glass and carbon fiber-reinforced composites by using nanosilica in the fiber sizing. (2017).
- [19] Tate, J. S., Akinola, A. T., Espinoza, S., Gaikwad, S., Kannabiran Vasudevan, D. K., Sprenger, S. and Kumar, K. Tension-tension fatigue performance and stiffness degradation of nanosilica-modified glass fiber-reinforced composites. *Journal of Composite Materials*, 52, 6 (2018), 823-834.
- [20] Jeffery, M. and Williams, J. DuPont-NASCAR Marketing. *Kellogg School of Management Cases* (2017).
- [21] Hossain, M. S., Hossain, M. S., Rahman, M. M., Chowdhury, A. and Khan, R. A. Fabrication and characterization of Kevlar fiber reinforced polypropylene based composite for civil applications. *Adv Mater*, 7, 4 (2018), 105-110.
- [22] Gupta, M. and Srivastava, R. Mechanical, thermal and water absorption properties of hybrid sisal/jute fiber reinforced polymer composite (2016).
- [23] Hashim, N., Abdul Majid, D. L., Zahari, R. and Yidris, N. Tensile properties of woven Carbon/Kevlar reinforced epoxy hybrid composite. *Trans Tech Publ.* (2017).
- [24] Dorado, A. A., Peralta, E. K., Carpio, E. V., Lozada, E. P. and Elepaño, A. R. Biodegradable corn starch/silica nanocomposite sheets for food packaging applications. *Trans Tech Publ.* (2017).
- [25] Gorrepati, S. R., Sharma, B., Vates, U., Phanden, R. K., Mussada, E. K., Saha, S., Mohammed, A., Bannaravuri, P. K. and Rao, G. B. Fabrication and bend testing of DHAK fiber composites. *Materials Today: Proceedings* (2020).
- [26] Chetty, S. The structural integrity of nanoclay filled epoxy polymer under cyclic loading. 2017.
- [27] Khodadadi, A., Liaghat, G., Ahmadi, H., Bahramian, A. R. and Razmkhah, O. Impact response of Kevlar/rubber composite. *Composites Science and Technology*, 184 (2019), 107880.
- [28] Bhanupratap, R. Study on characterization and sorption behavior of jute reinforced epoxy composite: Hybridization effect of Kevlar fabric. *Materials Today: Proceedings*, 27 (2020), 2017-2021.
- [29] Miah, M. Y., Bhattacharjee, S., Begum, A., Bhowmik, S., Islam, M. S., Gafur, A. and Islam, M. S. Fabrication and Characterization of Differently Laminated Jute Mat-PVC Composites. *MAYFEB Journal of Materials Science*, 1 (2017).